Semiorthogonal Space–Time Block Codes

Ngoc-Dũng Đào, *Member, IEEE*, and Chintha Tellambura, *Senior Member, IEEE*

***Abstract*—In this paper, a new class of full-diversity, rate-one space–time block codes (STBCs) called semiorthogonal algebraic space–time block codes (SAST codes) is proposed. SAST codes are delay optimal when the number of transmit antennas is even. The SAST codeword matrix has a generalized Alamouti structure where the transmitted symbols are replaced by circulant matrices and the commutativity of circulant matrices simplifies the detection of transmit symbols. SAST codes with maximal coding gain are constructed by using rate-one linear threaded algebraic space–time (LTAST) codes. Compared with LTSAT codes, SAST codes not only reduce the complexity of maximum-likelihood detection, but also provide remarkable performance gain. They also outperform other STBC with rate one or less. SAST codes also perform well with suboptimal detectors such as the vertical-Bell Laboratories layered space–time (V-BLAST) nulling and cancellation receiver. Finally, SAST codes attain nearly 100% of the Shannon capacity of open-loop multiple-input–single-output (MISO) channels.**

***Index Terms*—Alamouti code, circulant matrix, multiple-input–multiple-output (MIMO) capacity, space–time block codes (STBCs), threaded algebraic space–time (TAST) codes, transmit diversity.**

I. Introduction

SPACE–TIME BLOCK CODES (STBCs), as one of space–time (ST) techniques for multiple-input–multiple-output (MIMO) systems, have been extensively studied recently. They have been proposed for several current and future wireless standards [1]. One of the most well-known STBC is the Alamouti code, first designed for two transmit antennas [2] and later generalized as an orthogonal STBC (OSTBC) [3]. Orthogonal designs result in a decoupling of symbol detection, enabling minimal complexity maximum-likelihood (ML) detection. OSTBC is said to be single-symbol decodable [4]. However, orthogonality entails low code rates [5]; a code rate (defined by the average number of transmitted information symbols per channel use (pcu) [6]) of one symbol pcu with complex constellations is available for two transmit antennas only, and the code rate approaches $1/2$ for a large number of transmit antennas [5].

The code rate may be improved by using quasi-orthogonal STBC (QSTBC) [7], [8], which achieve full diversity by signal constellation rotations (see [9] and references therein), but require joint ML detection[1] of pairs of symbols (double-symbol decoding). Moreover, QSTBC also have low code rates because they are based on OSTBC. A novel code design framework, namely coordinate interleaved orthogonal design (CIOD), has been proposed in [4]. CIOD codes are also derived from OSTBC; the former however offer similar or higher rates than those of OSTBC and QSTBC, while the detection complexity is the same as OSTBC. For eight transmit antennas, another double-symbol decodable CIOD code of rate one is presented in [10]. Similar to QSTBC codes, CIOD codes require signal rotation to achieve full diversity.

On the other hand, full-diversity diagonal space–time (DST) codes are designed without considering the column orthogonality of codeword matrices [11], [12], and rate-one codes can thus be constructed for any number of transmit antennas. Optimal DST codes yield better coding gains compared to those of OSTBC for more than two transmit antennas. However, DST codes exhibit high peak-to-average-power ratio (PAPR). Therefore, linear threaded algebraic space–time (LTAST) codes have been proposed to reduce the PAPR of DST codes [13]. Rate-one LTAST codes have a circulant structure [14] and the same PAPR as the input constellation. Another framework to design high-rate codes is proposed in [15] by using division algebras. Specifically, a rate-one code is derived from field extensions and has γ-circulant structure [15, Sec. III.A.1]. DST, LTAST, and STBC from division algebras are all delay optimal in the sense that the number of channel uses per ST codeword equals to the number of transmit antennas; i.e., the ST codewords are square matrices [3]. However, their ML decoding complexity is much higher than that of QSTBC or CIOD codes since all the transmitted symbols must be jointly decoded.

In this paper, we present a new class of STBC called semiorthogonal algebraic space–time (SAST) codes for any number of transmit antennas. SAST codes are of rate one and achieve full diversity. The structure of SAST codes can be viewed as a generalization of the Alamouti code, where each data symbol is replaced by a circulant matrix. Hence, the left-half columns of the codeword matrices are orthogonal to the right-half columns. Consequently, each half of the input symbols can be ML detected separately. Therefore, the complexity of ML detection for SAST codes is remarkably less than that of rate-one LTAST codes. If the number of transmit antennas M is even, i.e., $M = 2m$, SAST codes are also delay optimal. Otherwise, the codes for $M = 2m - 1$ can

Manuscript received March 25, 2005; revised March 25, 2009. Current version published December 23, 2009. This work was supported by The National Sciences and Engineering Research Council (NSERC), Canada and by the Alberta Informatics Circle of Research Excellence (iCORE), Canada. The material in this paper was presented in part at the 2005 IEEE Global Telecommunications Conference, St. Louis, MO, November/December 2005.

N.-D. Đào was with the Department of Electrical and Computer Engineering, University of Alberta, Edmonton, AB T6G 2V4 Canada. He is now with Toshiba Research Europe, Ltd., Telecommunications Research Laboratory, Bristol, BS1 4ND, U.K. (e-mail: dndao@ieee.org).

C. Tellambura is with the Department of Electrical and Computer Engineering, University of Alberta, Edmonton, AB T6G 2V4 Canada (e-mail: chintha@ece.ualberta.ca).

Communicated by B. S. Rajan, Associate Editor for Coding Theory.

Digital Object Identifier 10.1109/TIT.2009.2034880

[1]We use the terms detection and decoding synonymously.

be obtained by deleting one column of the codes designed for $M = 2m$. SAST codes can achieve full diversity by proper signal designs, such as signal rotation techniques [13]. With its special structure, optimal rotations of different constellations for SAST codes are shown to be the ones designed for rate-one LTAST codes [13].

The idea of using the Alamouti code structure to build rate-one STBC, called extended Alamouti STBC, for $M = 2^k$ transmit antennas is also investigated in [16]. The extended Alamouti codes have a recursive structure, where a code for $M = 2^k$ is used to construct another code for $M = 2^{k+1}$. However, the codes do not achieve full diversity and have a low coding gain. In [17], the authors present another recursive rate-one STBC construction, in which one-half of the symbols are orthogonal to the other half, and each half can be decoded separately. While this feature is similar to that of our proposed codes, the authors' codes are not delay optimal for $M \neq 2^k$; therefore, these codes have higher decoding complexity than that of our codes for $M \neq 2^k, 2^k - 1$. Additionally, the coding gain is not maximized; thus, the performance of these codes may be inferior to that of our codes.

The paper is organized as follows. Section II describes the system model, provides necessary mathematical backgrounds for the design of SAST codes, and briefly reviews the properties of rate-one LTAST constellations. The design of SAST codes and their properties are given in Section III. The simulations results are discussed in Section IV. The conclusions and final remarks are presented in Section V.

II. Preliminaries

A. Notation

Superscripts T, $*$, and H denote matrix transpose, conjugate, and transpose conjugate operations. $\mathbb{E}[\cdot]$ denotes the statistical mean. A complex Gaussian random variable with mean m and variance σ^2 is denoted by $\mathcal{CN}(m, \sigma^2)$. A signal constellation U of μ points is a subset of the field of complex numbers $\mathbb{C}$; μ is called the order or size of U. The minimum Euclidean distance of U is $d_{\min} = \min\{|u - \hat{u}| \forall u \neq \hat{u}; u, \hat{u} \in \mathsf{U}\}$, where $|x|$ represents the absolute value of x. An element of U is called a signal or a symbol, and all the elements are equally likely to be transmitted. The average energy of a constellation is normalized such that $E[|u|^2] = 1$. For example, a square quadrature amplitude modulation (QAM) constellation can be represented as a set $\mathsf{U} = \{n_1 d_{\min} + j n_2 d_{\min} + u_0 | n_1, n_2 \in \mathbb{Z}, j^2 = -1, u_0 \text{ constant}\}$.

B. System Model

We consider data transmission over a quasi-static Rayleigh flat fading channel. The transmitter and receiver are equipped with M transmit and N receive antennas. The channel gain h_{ik} $(i = 1, 2, \ldots, M; k = 1, 2, \ldots, N)$ between the (i,k)th transmit–receive antenna pair is assumed to be $\mathcal{CN}(0, 1)$. We assume that there is no spatial correlation at either the transmit array or the receive array, and that the receiver, but not the transmitter, completely knows the channel gains.

The ST encoder maps data symbols into ST codewords $\mathbf{C} = [c_{ti}]$ of size $T \times M$ where c_{ti} is the symbol transmitted from antenna i at time t $(1 \leq t \leq T)$. The average energy of a codeword is constrained such that $\sum_{i=1}^{M} \sum_{t=1}^{T} \mathbb{E}[|c_{ti}|^2] = T$.

The received signals y_{tk} of kth antenna at time t can be arranged in a matrix $\mathbf{Y}$ of size $T \times N$. Thus, one can represent the transmit–receive signal relation compactly as

$$\mathbf{Y} = \sqrt{\rho}\mathbf{C}\mathbf{H} + \mathbf{Z} \tag{1}$$

where $\mathbf{H} = [h_{ik}]$, $\mathbf{Z} = [z_{tk}]$ of size $T \times N$, and z_{tk} are independently, identically distributed (i.i.d.) $\mathcal{CN}(0, 1)$. The transmit power is scaled by ρ so that the average signal-to-noise ratio (SNR) at each receive antenna is ρ, independent of the number of transmit antennas.

The upper bound of pair-wire error probability (PEP) derived by Tarokh *et al.* [6] is as follows:

$$\mathbf{P}(\mathbf{C} \to \hat{\mathbf{C}}) \leq \left(\prod_{i=1}^{\Gamma} \lambda_i \right)^{-N} \left(\frac{\rho}{4} \right)^{-\Gamma N} \tag{2}$$

where $\mathbf{C}$ and $\hat{\mathbf{C}}$ are the transmitted and erroneously decoded codewords, Γ is the minimum rank of a matrix $\mathbf{\Delta}_C$ $(\mathbf{\Delta}_C = \mathbf{C} - \hat{\mathbf{C}})$ for all $\mathbf{C} \neq \hat{\mathbf{C}}$, and $\lambda_1, \lambda_2, \ldots, \lambda_\Gamma$ are nonzero eigenvalues of a product matrix $\mathbf{P}_C = \mathbf{\Delta}_C^{\mathsf{H}} \mathbf{\Delta}_C$. We can define $d_c = (\prod_{i=1}^{\Gamma} \lambda_i)^{1/\Gamma}$ as a distance of two distinct ST codewords. The diversity gain or diversity order G_d and the coding gain G_c of the ST codes are defined as $G_d = \Gamma N$ and $G_c = \min_{\mathbf{C} \neq \hat{\mathbf{C}}} d_c = \min_{\mathbf{C} \neq \hat{\mathbf{C}}} (\prod_{i=1}^{\Gamma} \lambda_i)^{1/\Gamma}$, respectively. Since $\operatorname{rank} \mathbf{\Delta}_C = \operatorname{rank} \mathbf{P}_C$, if $\mathbf{\Delta}_C$ of an ST code is of full rank M for all pairs of distinct codewords, then so is the $\mathbf{P}_C$, and the diversity order is maximized; i.e., $G_d = MN$. In this case, the ST code is said to achieve full diversity. The coding gain follows $G_c = \min_{\mathbf{C} \neq \hat{\mathbf{C}}} [\det(\mathbf{\Delta}_C^{\mathsf{H}} \mathbf{\Delta}_C)]^{1/M}$.

For example, the coding gain of OSTBC is given by [9]

$$G_c^O = \frac{1}{M R_M} d_{\min}^2 \tag{3}$$

where R_M is the code rate of the OSTBC designed for M transmit antennas [9].[2] The multiplicative factor $\frac{1}{M R_M}$ appears because of the transmit power constraint. The maximal rate of OSTBC with the number of transmit antennas $M = 2a$ or $M = 2a - 1$ is given by $R_M = \frac{a+1}{2a}$ [5]. The optimal coding gain of QSTBC with even M transmit antennas can be derived as [9]

$$G_c^Q = \frac{1}{M R_{M/2}} d_{\min}^2. \tag{4}$$

Note that the coding gain is simply an asymptotic performance metric since it is defined for a worst case PEP basis and at high SNR. The actual performance of an ST code depends on the whole distance spectrum. Simulations are, therefore, required to compare the SNR gain of different ST codes.

C. Circulant Matrices

The circulant matrix [14] structure is proposed for rate-one LTAST codes in [13]. However, some interesting properties of circulant matrix are not exploited. We thus first review several

[2] In [9], the authors define a parameter ζ, namely, the diversity product. The coding gain can be calculated as $G_c = 4\zeta^2$.

properties of circulant matrices that will be employed to develop SAST codes.

A matrix $\mathcal{C} = [c_{ik}]$ is called a circulant matrix of order m

$$\mathcal{C} = \begin{bmatrix} x_1 & x_2 & \dots & x_m \\ x_m & x_1 & \dots & x_{m-1} \\ \vdots & \vdots & & \vdots \\ x_2 & x_3 & \dots & x_1 \end{bmatrix}. \tag{5}$$

Therefore, $c_{ik} = x_{(k-i+1) \bmod m}$. Since a circulant has only m independent entries, which are the elements of vector $\mathbf{x} = [x_1, x_2, \dots, x_m]$, we can write $\mathcal{C}(\mathbf{x})$ to emphasize that the first row of the circulant $\mathcal{C}$ is exactly the row vector $\mathbf{x}$. Other rows ith $(i = 2,3,\dots,m)$ are obtained by circular shifts to the right $(i-1)$ times of the vector $\mathbf{x}$. The basic properties of circulants are given as follows.

- P1) $\mathcal{C}$ is a circulant if and only if $\mathcal{C}^\dagger$ is a circulant.
- P2) If $\mathcal{A}$ and $\mathcal{B}$ are circulants of order m, and α_1 and α_2 are two scalars, then the matrices $\mathcal{A}^\mathsf{T}$, $\alpha_1\mathcal{A} + \alpha_2\mathcal{B}$, $\mathcal{A}\mathcal{B}$ are circulants.
- P3) All circulants of the same order commute, i.e., $\mathcal{A}\mathcal{B} = \mathcal{B}\mathcal{A}$.
- P4) Let $\mathbf{F}$ be a Fourier transform matrix with $f_{i,k} = \frac{1}{\sqrt{m}} e^{-j2\pi(i-1)(k-1)/m}$, where $j^2 = -1$. If $\mathcal{C}$ is a circulant, it is diagonalized by $\mathbf{F}$: $\mathcal{C} = \mathbf{F}^\mathsf{H}\mathbf{\Lambda}\mathbf{F}$, where $\mathbf{\Lambda} = \mathrm{diag}[\lambda_1, \lambda_2, \dots, \lambda_m]$, and λ_i is the eigenvalue of $\mathcal{C}$.
- P5) The eigenvalues of a circulant are the Fourier transform of the first row of the circulant as $[\lambda_1, \lambda_2, \dots, \lambda_m]^\mathsf{T} = \sqrt{m}\mathbf{F}\mathbf{x}^\mathsf{T}$. Thus, any order-$m$ circulant always has m distinct eigenvectors, which are the columns of the Fourier transform matrix. However, the number of eigenvalues may be less than m.

Another type of circulant matrix is the left circulant [14] that we can denote by $\mathcal{C}^L(\mathbf{x})$, where the ith row is obtained by circular shifts $(i-1)$ times to the left vector $\mathbf{x}$

$$\mathcal{C}^L(\mathbf{x}) = \begin{bmatrix} x_1 & x_2 & \dots & x_m \\ x_2 & x_3 & \dots & x_1 \\ \vdots & \vdots & & \vdots \\ x_m & x_1 & \dots & x_{m-1} \end{bmatrix}. \tag{6}$$

Let a permutation Π on an arbitrary matrix X be such that the $(m-i+2)$th row is permuted with the ith row for $i = 2,3,\dots,\lceil \frac{m}{2} \rceil$, where $\lceil(\cdot)\rceil$ is the ceiling function. One can verify that

$$\Pi(\mathcal{C}^L(\mathbf{x})) = \mathcal{C}(\mathbf{x}). \tag{7}$$

This useful operator will be used for our derivation.

D. Linear Threaded Algebraic Space–Time Constellations

We briefly review the code construction and properties of rate-one LTAST codes. For a full treatment of LTAST codes, the reader is referred to [13] and the references therein. For brevity, we use the term LTAST codes to denote the rate-one LTAST codes when there is no ambiguity.

Let m be the number of transmit antennas. Modulation symbols are drawn from a constellation S with the minimum Euclidean distance $d_{\min}$ and arranged in a vector $\mathbf{s} = [s_1, s_2, \dots, s_m]^\mathsf{T}$. The transmitted vector $\mathbf{u}$ is given by

$$\mathbf{u} = \mathbf{R}\mathsf{s} \tag{8}$$

where $\mathbf{R} = \mathrm{diag}[1,\ \phi^{1/m},\ \dots,\ \phi^{(m-1)/m}]$ and ϕ is called a Diophantine number [13]. LTAST codewords are circulants given by

$$\mathbf{D} = \frac{1}{\sqrt{m}}\mathcal{C}(\mathbf{u}^\mathsf{T}). \tag{9}$$

The upper bound of coding gain is as follows.

Proposition 1 [13, eq. (7)]: The coding gain of the rate-one LTAST codes is upper bounded by $G_c^L \le \frac{1}{m} d_{\min}^2$.

To ensure the codes achieve full diversity, the Diophantine number is chosen as $\phi = e^{j\alpha}$. Thus, the ith symbol s_i is rotated by an angle $\frac{i-1}{m}\alpha$. The optimal values of ϕ that maximize the coding gain are specified in [13, Th. 2].

Proposition 2: For $m = 2^r, r \ge 1$, the optimal coding gain of rate-one LTAST codes, i.e., $G_C^L = \frac{1}{m} d_{\min}^2$, can be obtained by choosing the Diophantine number $\phi = j$ $(j^2 = -1)$ and constellations $\mathcal{S}$ carved from the ring of Gaussian integers, and for $m = 2^{r_0}3^{r_1}, r_0, r_1 \ge 0$ by choosing $\phi = e^{2j\pi/6}$ and constellations $\mathcal{S}$ carved from the ring of Einstein integers.

Note that the constellations carved from the ring of Gaussian integers include QAM constellations, while the constellations carved from the ring of Einstein integers include hexagonal constellations [18]. In [13, Th. 1], it was also suggested how to select ϕ for PSK constellations; however, a computer search is required to find the ϕ that maximizes the coding gain. Additionally, for $m \ne 2^r$ or $m = 2^{r_0}3^{r_1}$, only local maxima of the coding gain are certain to be found by a computer search.

Full diversity for LTAST codes is achieved when the m transmitted symbols are jointly ML detected, for example, by a sphere decoder [19]. Therefore, the decoding complexity of the LTAST codes is higher than that of OSTBC for $m > 1$. Additionally, Proposition 1 shows that the coding gain decreases when m increases.

In the next section, we will present our new SAST codes by using a block circulant structure. Constellation rotation is needed to achieve full diversity as is the case for LTAST codes. However, SAST codes exploit the commutativity of circulant matrices and, hence, yield significant improvements over LTAST codes.

III. SAST Code Construction and Properties

A. Encoder

We consider the number of transmit antennas is $M = 2m$. The SAST codeword designed for M transmit antennas is formulated as follows:

$$\mathcal{S}_M = \kappa \begin{bmatrix} \mathbf{A} & \mathbf{B} \\ -\mathbf{B}^\mathsf{H} & \mathbf{A}^\mathsf{H} \end{bmatrix} \tag{10}$$

where $\mathbf{A}$ and $\mathbf{B}$ are two $m \times m$ circulant matrices generated by two input data vectors $\mathbf{s}_1$ and $\mathbf{s}_2$, and each consists of m

information symbols drawn from the same signal constellation. $\kappa = 1/\sqrt{M}$ is a power normalization constant. We sometimes omit κ for brevity, where no confusion may arise. In principle, $\mathbf{A}$ and $\mathbf{B}$ can be considered as two $m \times m$ codewords of rate-one LTAST codes. We do not have to restrict ourselves to the optimal rotations of the LTAST codes given in Proposition 2. The only requirement is that the building LTAST codes of size $m \times m$ are full diversity. To satisfy this requirement, input vectors are first rotated by the same rotation matrix $\mathbf{R}$ such that $\mathbf{u}_1 = \mathbf{R}\mathbf{s}_1$ and $\mathbf{u}_2 = \mathbf{R}\mathbf{s}_2$; then the rotated vectors are used to generate two LTAST codewords of size m $\mathbf{A} = \mathcal{C}(\mathbf{u}_1^{\mathsf{T}})$ and $\mathbf{B} = \mathcal{C}(\mathbf{u}_2^{\mathsf{T}})$.

Our structure of SAST codes is different from that of the QSTBC proposed by Jafarkhani [7] with a codeword matrix $\begin{bmatrix} \mathbf{A} & \mathbf{B} \\ -\mathbf{B}^* & \mathbf{A}^* \end{bmatrix}$, where $\mathbf{A}$ and $\mathbf{B}$ are conjugated, but not conjugate transposed as SAST codes. SAST codes' structure is also different from the QSTBC structure introduced by Tirkkonen *et al.* [8], where the codeword is $\begin{bmatrix} \mathbf{A} & \mathbf{B} \\ \mathbf{B} & \mathbf{A} \end{bmatrix}$. Furthermore, in both these QSTBC structures, $\mathbf{A}$ and $\mathbf{B}$ are OSTBC codewords of the same size, but are not the circulant matrices. Hence, these QSTBC are rate one for $M = 3, 4$ only, whereas SAST codes are rate one for any number of antennas.

The SAST codes for four and six antennas are given as the following examples:

$$\mathcal{S}_4 = \frac{1}{2}\begin{bmatrix} u_1 & u_2 & u_3 & u_4 \\ u_2 & u_1 & u_4 & u_3 \\ -u_3^* & -u_4^* & u_1^* & u_2^* \\ -u_4^* & -u_3^* & u_2^* & u_1^* \end{bmatrix}$$

$$\mathcal{S}_6 = \frac{1}{\sqrt{6}}\begin{bmatrix} u_1 & u_2 & u_3 & u_4 & u_5 & u_6 \\ u_3 & u_1 & u_2 & u_6 & u_4 & u_5 \\ u_2 & u_3 & u_1 & u_5 & u_6 & u_4 \\ -u_4^* & -u_6^* & -u_5^* & u_1^* & u_3^* & u_2^* \\ -u_5^* & -u_4^* & -u_6^* & u_2^* & u_1^* & u_3^* \\ -u_6^* & -u_5^* & -u_4^* & u_3^* & u_2^* & u_1^* \end{bmatrix}.$$

B. Properties of SAST Codes

As the most important design criterion, the diversity gain of SAST codes is first analyzed.

Lemma 1: SAST codes achieve full diversity for quasi-static channels if the building LTAST codes have full diversity.

Proof: Let $\mathbf{S}$ and $\hat{\mathbf{S}}$ be two distinct SAST codewords; then the product matrix $\mathbf{P}_S = \mathbf{\Delta}_S^{\mathsf{H}}\mathbf{\Delta}_S$ is given by

$$\begin{aligned}\mathbf{P}_S &= \frac{1}{M}\mathbf{\Delta}_S^{\mathsf{H}}\mathbf{\Delta}_S \\ &= \begin{bmatrix} \mathbf{\Delta}_A^{\mathsf{H}}\mathbf{\Delta}_A + \mathbf{\Delta}_B^{\mathsf{H}}\mathbf{\Delta}_B & \mathbf{\Delta}_A^{\mathsf{H}}\mathbf{\Delta}_B - \mathbf{\Delta}_B\mathbf{\Delta}_A^{\mathsf{H}} \\ \mathbf{\Delta}_B^{\mathsf{H}}\mathbf{\Delta}_A - \mathbf{\Delta}_A\mathbf{\Delta}_B^{\mathsf{H}} & \mathbf{\Delta}_A^{\mathsf{H}}\mathbf{\Delta}_A + \mathbf{\Delta}_B^{\mathsf{H}}\mathbf{\Delta}_B \end{bmatrix} \\ &= \frac{1}{M}\begin{bmatrix} \mathbf{P}_A + \mathbf{P}_B & \mathbf{0}_m \\ \mathbf{0}_m & \mathbf{P}_A + \mathbf{P}_B \end{bmatrix} \end{aligned} \tag{11}$$

where $\mathbf{\Delta}_A = \mathbf{A} - \hat{\mathbf{A}}$, $\mathbf{\Delta}_B = \mathbf{B} - \hat{\mathbf{B}}$, $\mathbf{P}_A = \mathbf{\Delta}_A^{\mathsf{H}}\mathbf{\Delta}_A$, and $\mathbf{P}_B = \mathbf{\Delta}_B^{\mathsf{H}}\mathbf{\Delta}_B$, and $\mathbf{0}_m$ denotes the $m \times m$ all-zero matrix. The second line of (11) comes from the property P3) of circulant matrices.

For two distinct codewords, at least either $\mathbf{A} \neq \hat{\mathbf{A}}$ or $\mathbf{B} \neq \hat{\mathbf{B}}$. Thus, at least one of the matrices $\mathbf{P}_A$ and $\mathbf{P}_B$ is full rank or they both are full rank because $\mathbf{A}$ and $\mathbf{B}$ are the codewords of the LTAST codes. Equivalently, at least one of $\mathbf{P}_A$ or $\mathbf{P}_B$ or they are both positive-definite matrices. Without loss of generality, we assume that $\mathbf{P}_A$ is positive definite. Let $\lambda_k(\mathbf{P}_A + \mathbf{P}_B)$, $\lambda_k(\mathbf{P}_A)$, and $\lambda_k(\mathbf{P}_B)$ $(k = 1, 2, \ldots, m)$ be the eigenvalues of matrices $(\mathbf{P}_A + \mathbf{P}_B)$, $\mathbf{P}_A$, and $\mathbf{P}_B$, respectively, arranged in nondecreasing order. Then, $\lambda_k(\mathbf{P}_A) \neq 0\ \forall k = 1, 2, \ldots, m$. From [20, Th. 7.2.1, p. 402], we have

$$\lambda_k(\mathbf{P}_A + \mathbf{P}_B) \geq \lambda_k(\mathbf{P}_A) + \lambda_1(\mathbf{P}_B) \geq \lambda_k(\mathbf{P}_A) > 0. \tag{12}$$

Consequently, $\det(\mathbf{P}_S) = \left(\frac{1}{M}\right)^M [\det(\mathbf{P}_A + \mathbf{P}_B)]^2 \geq \left(\frac{1}{M}\right)^M [\det(\mathbf{P}_A)]^2 > 0$. Thus, the matrix $\mathbf{P}_S$ is always full rank for all input symbols, and the SAST block codes achieve full diversity. □

Now we consider the coding gain of the SAST block codes. In the worst case, $\min[\det(\mathbf{P}_S)]^{1/M} = \frac{1}{M}\min[\det(\mathbf{P}_A)]^{2/M}$. With reference to Proposition 1, the coding gain of SAST codes is $G_c^S = \min[\det(\mathbf{P}_S)]^{1/M} = \frac{1}{M}\min[\det(\mathbf{P}_A)]^{2/M}$. Note that $M = 2m$, and that $\frac{1}{m}\min[\det(\mathbf{P}_A)]^{1/m}$ is actually the coding gain of the LTAST codes for m antennas, which is $d_{\min}^2/m$. Hence, $G_c^S = \frac{1}{2m}d_{\min}^2 = \frac{1}{M}d_{\min}^2$, which turns out to be the coding gain of the LTAST codes for M antennas. We thus have the following Lemma for the coding gain of SAST codes.

Lemma 2: The coding gain of SAST codes is equal to that of the rate-one LTAST codes for the same $M = 2m$ transmit antennas and is upper bounded by $G_c^S \leq \frac{1}{M}d_{\min}^2$.

Lemma 2 shows that optimal rotation angles of the LTAST codes are also optimal for SAST codes. Although the two codes have the same coding gain, SAST codes have a much better distance spectrum compared with the LTAST codes, and thus, the former has a much better performance, as we will demonstrate in our investigation of simulation results in Section IV. We next show that this improvement comes without any extra detection complexity, and, better still, that the ML detection complexity reduces.

C. SAST Detector

Since detection of transmit symbols is an essential part of the system, we will derive the detectors for SAST codes and show how to reduce the detection complexity.

We initially consider one receive antenna $N = 1$. If $N > 1$, we can perform maximal ratio combining (MRC) for the received signals of each receive antenna, and the decoder for one receive antenna can still be employed.

Let $\mathbf{y} = [\mathbf{y}_1^{\mathsf{T}}\ \mathbf{y}_2^{\mathsf{T}}]^{\mathsf{T}}$, $\mathbf{y}_1 = [y_1, y_2, \ldots, y_m]^{\mathsf{T}}$, $\mathbf{y}_2 = [y_{m+1}, y_{m+2}, \ldots, y_{2m}]^{\mathsf{T}}$, $\mathbf{h} = [\mathbf{h}_1^{\mathsf{T}}\ \mathbf{h}_2^{\mathsf{T}}]^{\mathsf{T}}$, $\mathbf{h}_1 = [h_1, h_2, \ldots, h_m]^{\mathsf{T}}$, $\mathbf{h}_2 = [h_{m+1}, h_{m+2}, \ldots, h_{2m}]^{\mathsf{T}}$, $\mathbf{z} = [\mathbf{z}_1^{\mathsf{T}}\ \mathbf{z}_2^{\mathsf{T}}]^{\mathsf{T}}$, $\mathbf{z}_1 = [z_1, z_2, \ldots, z_m]^{\mathsf{T}}$, and $\mathbf{z}_2 = [z_{m+1}, z_{m+2}, \ldots, z_{2m}]^{\mathsf{T}}$; then we obtain

$$\begin{bmatrix} \mathbf{y}_1 \\ \mathbf{y}_2 \end{bmatrix} = \begin{bmatrix} \mathbf{A} & \mathbf{B} \\ -\mathbf{B}^{\mathsf{H}} & \mathbf{A}^{\mathsf{H}} \end{bmatrix}\begin{bmatrix} \mathbf{h}_1 \\ \mathbf{h}_2 \end{bmatrix} + \begin{bmatrix} \mathbf{z}_1 \\ \mathbf{z}_2 \end{bmatrix}. \tag{13}$$

An equivalent form of (13) is

$$\begin{bmatrix} \mathbf{y}_1 \\ \mathbf{y}_2^* \end{bmatrix} = \begin{bmatrix} \mathbf{X}_1 & \mathbf{X}_2 \\ \mathbf{X}_3 & \mathbf{X}_4 \end{bmatrix}\begin{bmatrix} \mathbf{u}_1 \\ \mathbf{u}_2 \end{bmatrix} + \begin{bmatrix} \mathbf{z}_1 \\ \mathbf{z}_2^* \end{bmatrix} \tag{14}$$

where

$$\mathbf{X}_1 = \begin{bmatrix} h_1 & h_2 & \cdots & h_m \\ h_2 & h_3 & \cdots & h_1 \\ \vdots & \vdots & \ddots & \vdots \\ h_m & h_1 & \cdots & h_{m-1} \end{bmatrix} = \mathcal{C}^L(\mathbf{h}_1^{\mathsf{T}})$$

$$\mathbf{X}_2 = \begin{bmatrix} h_{m+1} & h_{m+2} & \cdots & h_{2m} \\ h_{m+2} & h_{m+3} & \cdots & h_{m+1} \\ \vdots & \vdots & \ddots & \vdots \\ h_{2m} & h_{m+1} & \cdots & h_{2m-1} \end{bmatrix} = \mathcal{C}^L(\mathbf{h}_2^{\mathsf{T}})$$

$$\mathbf{X}_3 = \begin{bmatrix} h_{m+1}^* & h_{2m}^* & \cdots & h_{m+2}^* \\ h_{m+2}^* & h_{m+1}^* & \cdots & h_{m+3}^* \\ \vdots & \vdots & \ddots & \vdots \\ h_{2m}^* & h_{2m-1}^* & \cdots & h_{m+1}^* \end{bmatrix} = \mathcal{C}^{\mathsf{H}}(\mathbf{h}_2^{\mathsf{T}})$$

$$\mathbf{X}_4 = -\begin{bmatrix} h_1^* & h_m^* & \cdots & h_2^* \\ h_2^* & h_1^* & \cdots & h_3^* \\ \vdots & \vdots & \ddots & \vdots \\ h_m^* & h_{m-1}^* & \cdots & h_{1^{\mathsf{T}}}^* \end{bmatrix} = -\mathcal{C}^{\mathsf{H}}(\mathbf{h}_1^{\mathsf{T}}).$$

By using (14), two vectors $\mathbf{u}_1$ and $\mathbf{u}_2$ can be jointly detected by, for example, a sphere decoder. However, the joint detectors result in the same complexity as that of the LTAST decoders. Next, we will show how to reduce the detection complexity.

Applying permutation Π (defined in Section II-B) for the column matrix $\mathbf{y}_1$, we obtain

$$\begin{aligned} \begin{bmatrix} \bar{\mathbf{y}}_1 \\ \bar{\mathbf{y}}_2 \end{bmatrix} &= \begin{bmatrix} \Pi(\mathbf{y}_1) \\ \mathbf{y}_2^* \end{bmatrix} \\ &= \begin{bmatrix} \Pi(\mathbf{X}_1) & \Pi(\mathbf{X}_2) \\ \mathbf{X}_3 & \mathbf{X}_4 \end{bmatrix} \begin{bmatrix} \mathbf{u}_1 \\ \mathbf{u}_2 \end{bmatrix} + \begin{bmatrix} \Pi(\mathbf{z}_1) \\ \mathbf{z}_2^* \end{bmatrix} \\ &= \underbrace{\begin{bmatrix} \mathbf{H}_1 & \mathbf{H}_2 \\ \mathbf{H}_2^{\mathsf{H}} & -\mathbf{H}_1^{\mathsf{H}} \end{bmatrix}}_{\mathbf{H}} \begin{bmatrix} \mathbf{u}_1 \\ \mathbf{u}_2 \end{bmatrix} + \begin{bmatrix} \bar{\mathbf{z}}_1 \\ \bar{\mathbf{z}}_2 \end{bmatrix} \end{aligned} \tag{15}$$

where $\bar{\mathbf{y}}_1 = \Pi(\mathbf{y}_1)$, $\bar{\mathbf{y}}_2 = \mathbf{y}_2^*$, $\mathbf{H}_1 = \mathcal{C}(\mathbf{h}_1^{\mathsf{T}})$, $\mathbf{H}_2 = \mathcal{C}(\mathbf{h}_2^{\mathsf{T}})$, $\bar{\mathbf{z}}_1 = \Pi(\mathbf{z}_1)$, and $\bar{\mathbf{z}}_2 = \mathbf{z}_2^*$. The elements of $\bar{\mathbf{z}}_1$ and $\bar{\mathbf{z}}_2$ have the same statistics $\mathcal{CN}(0,1)$ as the elements of $\mathbf{z}_1$ and $\mathbf{z}_2$. We now perform MRC by left multiplying $\mathbf{H}^{\mathsf{H}}$ to both sides of (15). Let $\hat{\mathbf{H}} = \mathbf{H}_1^{\mathsf{H}}\mathbf{H}_1 + \mathbf{H}_2^{\mathsf{H}}\mathbf{H}_2$; then we get

$$\begin{aligned} \begin{bmatrix} \hat{\mathbf{y}}_1 \\ \hat{\mathbf{y}}_2 \end{bmatrix} &= \mathbf{H}^{\mathsf{H}} \begin{bmatrix} \bar{\mathbf{y}}_1 \\ \bar{\mathbf{y}}_2 \end{bmatrix} = \begin{bmatrix} \hat{\mathbf{H}} & \mathbf{0}_m \\ \mathbf{0}_m & \hat{\mathbf{H}} \end{bmatrix} \begin{bmatrix} \mathbf{u}_1 \\ \mathbf{u}_2 \end{bmatrix} + \mathbf{H}^{\mathsf{H}} \begin{bmatrix} \bar{\mathbf{z}}_1 \\ \bar{\mathbf{z}}_2 \end{bmatrix} \\ &= \begin{bmatrix} \hat{\mathbf{H}} & \mathbf{0}_m \\ \mathbf{0}_m & \hat{\mathbf{H}} \end{bmatrix} \begin{bmatrix} \mathbf{u}_1 \\ \mathbf{u}_2 \end{bmatrix} + \underbrace{\begin{bmatrix} \hat{\mathbf{z}}_1 \\ \hat{\mathbf{z}}_2 \end{bmatrix}}_{\hat{\mathbf{z}}}. \end{aligned} \tag{16}$$

The covariance matrix of the additive noise vector $\hat{\mathbf{z}}$ is

$$E[\mathbf{z}\mathbf{z}^{\mathsf{H}}] = \begin{bmatrix} \hat{\mathbf{H}} & \mathbf{0}_m \\ \mathbf{0}_m & \hat{\mathbf{H}} \end{bmatrix}. \tag{17}$$

Therefore, the noise vectors $\hat{\mathbf{z}}_1$ and $\hat{\mathbf{z}}_2$ are uncorrelated and have the same covariance matrix $\hat{\mathbf{H}}$. Thus, $\mathbf{u}_1$ and $\mathbf{u}_2$ can be detected separately by using $\hat{\mathbf{y}}_i = \hat{\mathbf{H}}\mathbf{u}_i + \hat{\mathbf{z}}_i$, $i = 1, 2$.

If there are $N > 1$ receive antennas, we have N matrices $\hat{\mathbf{H}}_k$ for $k = 1, 2, \ldots, N$, N received vectors $\hat{\mathbf{y}}_{ik}$, and N noise vectors $\hat{\mathbf{z}}_{ik}$. Let $\check{\mathbf{y}}_i = \sum_{k=1}^N \hat{\mathbf{y}}_{i,k}$, $\check{\mathbf{H}}_i = \sum_{k=1}^N \hat{\mathbf{H}}_k$, and $\check{\mathbf{z}}_i = \sum_{k=1}^N \hat{\mathbf{z}}_{ik}$; then the following equations can be used to detect the data vectors:

$$\check{\mathbf{y}}_i = \check{\mathbf{H}}_i \mathbf{u}_i + \check{\mathbf{z}}_i, \qquad \text{for } i = 1, 2. \tag{18}$$

The noise vectors $\check{\mathbf{z}}_1$ and $\check{\mathbf{z}}_2$ can be whitened by using the same whitening matrix $(\check{\mathbf{H}})^{-1/2}$. Finally, we obtain

$$\tilde{\mathbf{y}}_i = \check{\mathbf{H}}^{-1/2}\hat{\mathbf{y}}_i = \underbrace{\check{\mathbf{H}}^{1/2}\mathbf{R}}_{\tilde{\mathbf{H}}}\mathbf{s}_i + \underbrace{\check{\mathbf{H}}^{-1/2}\check{\mathbf{z}}_i}_{\tilde{\mathbf{z}}_i}, \qquad i = 1, 2. \tag{19}$$

Any detectors for the LTAST codes such as the optimum sphere decoder [19], vertical-Bell Laboratories layered space–time (V-BLAST) successive nulling, and cancellation [21] can be employed for the decoding of the SAST codes. However, two data vectors $\mathbf{s}_1$ and $\mathbf{s}_2$ can be detected in parallel. On average, the ML detection complexity of SAST codes reduces largely compared with that of that rate-one LTAST codes (Section IV).

D. Maximum Mutual Information

We now study the maximum mutual information of SAST codes over $(M, 1)$ multiple-input–single-output (MISO) channels. The equivalent channel $\mathbf{H}$ given in (15) can be used to calculate the maximum mutual information [22] of SAST codes as

$$\mathsf{C}_S = \frac{1}{M} E\left[\log_2 \det\left(\mathbf{I}_M + \frac{\rho}{M}\mathbf{H}\mathbf{H}^{\mathsf{H}}\right)\right]. \tag{20}$$

The normalizing factor $\frac{1}{M}$ is used to account for M channel uses. Note that $M = 2m$. Since $\mathbf{H}_1$ and $\mathbf{H}_2$ are circulant matrices, we have $\mathbf{H}\mathbf{H}^{\mathsf{H}} = \mathbf{H}^{\mathsf{H}}\mathbf{H} = \begin{bmatrix} \hat{\mathbf{H}} & \mathbf{0}_m \\ \mathbf{0}_m & \hat{\mathbf{H}} \end{bmatrix}$, where $\hat{\mathbf{H}} = \mathbf{H}_1\mathbf{H}_1^{\mathsf{H}} + \mathbf{H}_2\mathbf{H}_2^{\mathsf{H}}$ is also a circulant matrix of size $m \times m$. Using property P4) of circulant matrices, we have $\mathbf{F}^{\mathsf{H}}\hat{\mathbf{H}}\mathbf{F} = \mathrm{diag}[\hat{\lambda}_1, \hat{\lambda}_2, \ldots, \hat{\lambda}_m]$, where $\hat{\lambda}_i$'s are the eigenvalues of $\hat{\mathbf{H}}$. Therefore, $\hat{\lambda}_k = |\lambda_{1,k}|^2 + |\lambda_{2,k}|^2$ $(k = 1, 2, \ldots, m)$, where $\lambda_{1,k}$ and $\lambda_{2,k}$ are eigenvalues of $\mathbf{H}_1$ and $\mathbf{H}_2$, respectively. From property P5) of circulant matrices, we get $[\lambda_{i,1}, \lambda_{i,2}, \ldots, \lambda_{i,m}]^{\mathsf{T}} = \sqrt{m}\mathbf{F}\mathbf{h}_i$ $(i = 1, 2)$, and each $\lambda_{i,k}$ has distribution $\mathcal{CN}(0, m)$. Let $\hbar_{i,k} = \sqrt{m}\lambda_{i,k}$; then $\hbar_{i,k} \sim \mathcal{CN}(0, 1)$. We obtain a new expression for the maximum mutual information C_S as

$$\begin{aligned} \mathsf{C}_S &= \frac{2}{M} E\left[\log_2 \det\left(\mathbf{I}_{M/2} + \frac{\rho}{M}\hat{\mathbf{H}}\hat{\mathbf{H}}^{\mathsf{H}}\right)\right] \\ &= \frac{2}{M} E\Big\{\log_2 \det\Big[\mathbf{I}_{M/2} \\ &\qquad + \frac{\rho}{M}\mathrm{diag}\left(|\hat{\lambda}_1|^2, |\hat{\lambda}_2|^2, \ldots, |\hat{\lambda}_{M/2}|^2\right)\Big]\Big\} \\ &= E\left\{\log_2 \det\left[1 + \frac{\rho}{2}\left(|\hbar_{1,k}|^2 + |\hbar_{2,k}|^2\right)\right]\right\} \end{aligned} \tag{21}$$

where the subindex k can take one of the values of $1, 2, \ldots, M/2$, and, without loss of generality, k can be omitted. This expression is exactly the maximum mutual information of the Alamouti code (cf., [23, eq. (9)]). In other words, the maximum mutual information of SAST codes is constant with respect to the number of transmit antennas and is the open-loop capacity of a $(2, 1)$ MISO Rayleigh fading channel.

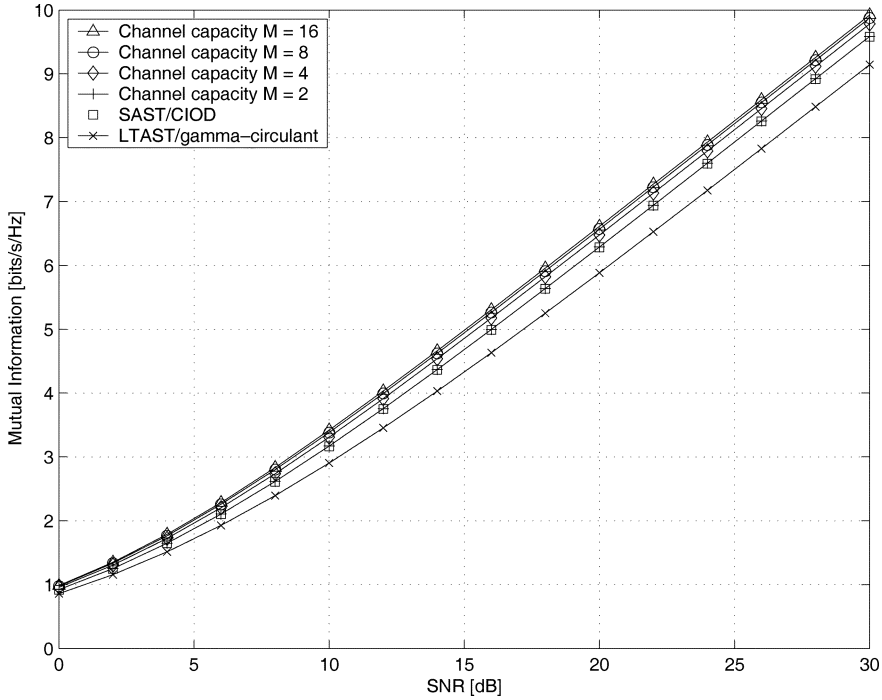

Fig. 1. Channel capacity and maximum mutual information of SAST and some other codes over open-loop MISO channels.

Let $\mathbf{h} = [\mathbf{h}_1^{\mathsf{T}}\ \mathbf{h}_2^{\mathsf{T}}]^{\mathsf{T}}$ and $\mathbf{H}_L = \mathcal{C}(\mathbf{h}^{\mathsf{T}})$, then by similar derivation steps as those for SAST codes, the maximum mutual information of the LTAST codes can be shown as

$$\begin{aligned}\mathsf{C}_L &= \frac{1}{M} E\left[\log_2 \det\left(\mathbf{I}_M + \frac{\rho}{M}\mathbf{H}_L\mathbf{H}_L^{\mathsf{H}}\right)\right] \\ &= E\left[\log_2 \det\left(1+\rho|\hbar|^2\right)\right] \end{aligned} \tag{22}$$

where $\hbar \sim \mathcal{CN}(0,1)$. Thus, the maximum mutual information of the LTAST codes is also constant with respect to the number of transmit antennas and is equal only to the open-loop capacity of the single-input–single-output (SISO) Rayleigh fading channel. This behavior is similar to that of the rate-one γ-circulant codes [15, p. 2605]. Clearly, the maximum mutual information of the LTAST and γ-circulant codes is less than that of SAST codes.

Fig. 1 illustrates the maximum mutual information of the SAST, LTAST, γ-circulant, and the rate-one CIOD codes for four antennas [4, eq. (132)] and eight antennas [10], together with the capacity of the MISO channels for $M = 2, 4, 8, 16$. In fact, SAST codes achieve the same channel capacity as that of the aforementioned CIOD codes, and this capacity is higher than that of the LTAST and γ-circulant codes.

To provide a closer comparison, the relative channel capacities attained by the SAST and LTAST codes are presented in Fig. 2. For $M = 4$, SAST codes reach more than 95% and up to 98% of the channel capacity. For $M = 16$, SAST codes achieve no less than about 92% channel capacity. This result occurs because for a specific high SNR, the channel capacity does not actually increase when the number of transmit antennas keeps growing, but the number of receive antennas is fixed [24]. Fig. 1 also shows that the capacity increment of the MISO channel is negligible when the number of transmit antennas increases from eight to 16. Therefore, the SAST codes nearly attain the capacity of the MISO channels.

If we consider the MIMO Rayleigh fading channels, i.e., the number of receive antennas $N > 1$, the maximum mutual information of the SAST and LTAST codes can be shown as follows:

$$\begin{aligned}&\mathsf{C}_S(\rho, M, N) \\ &\quad = E\left\{\log_2 \det\left[1 + \frac{\rho}{2}\sum_{k=1}^{N}\left(|\hbar_{1,k}|^2 + |\hbar_{2,k}|^2\right)\right]\right\} \end{aligned} \tag{23}$$

$$\begin{aligned}&\mathsf{C}_L(\rho, M, N) \\ &\quad = E\left[\log_2 \det\left(1 + \rho\sum_{k=1}^{N}|\hbar_k|^2\right)\right]. \end{aligned} \tag{24}$$

Arguments ρ, M, N are used to highlight the operation SNR and the antenna configuration. Let $\mathsf{C}(\rho, M, N)$ be the capacity of (M, N) MIMO channels. We can compare the maximum mutual information of SAST and LTAST codes with the channel capacity [23] as follows:

$$\begin{aligned}&\mathsf{C}_S(\rho, M, N) = \mathsf{C}(N\rho, 2N, 1) < \mathsf{C}(\rho, M, N) \\ &\mathsf{C}_L(\rho, M, N) = \mathsf{C}(\rho, 1, N) = \mathsf{C}(N\rho, N, 1) < \mathsf{C}_S(\rho, M, N).\end{aligned}$$

The two codes have a significant capacity loss if they are used in the MIMO Rayleigh fading channels. This result is not surprising, because the SAST and rate-one LTAST codes support only 1 symbol pcu, while the maximum multiplexing capacity is M symbols pcu. Nevertheless, the rate loss of SAST codes is always smaller than that of the rate-one LTAST codes.

Before investigating the bit error rate (BER) performance of SAST codes in the next section, we summarize the main parameters of SAST codes and compare them with several existing ST codes, including OSTBC, CIOD, QSTBC, and rate-one TAST/

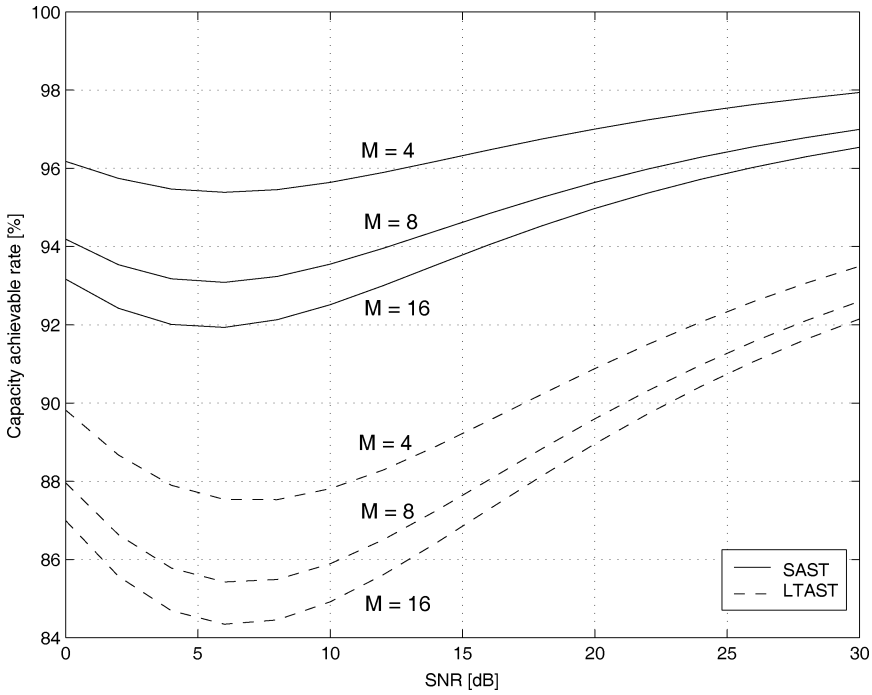

Fig. 2. Capacity achievable rates of SAST and LTAST codes compared with the capacity of open-loop MISO channels.

TABLE I
COMPARISONS OF SEVERAL STBC FOR $(4, N)$ SYSTEMS

Code	G_d	G_c	R	ML decoding	DO
OSTBC	$4N$	$\frac{1}{3}\,d^2_{\min}$	0.75	1 symbol	3
CIOD [4]	$4n$	$\frac{1}{2\sqrt{5}}\,d^2_{\min}$	1	1 symbols	3
QSTBC	$4N$	$\frac{1}{4}\,d^2_{\min}$	1	2 symbols	2
LTAST	$4N$	$\frac{1}{4}\,d^2_{\min}$	1	4 symbols	0
SAST	$4N$	$\frac{1}{4}\,d^2_{\min}$	1	2 symbols	2

TABLE II
COMPARISONS OF SEVERAL STBC FOR $(8, N)$ SYSTEMS

Code	G_d	G_c	R	ML decoding	DO
OSTBC	$8N$	$\frac{1}{5}d^2_{\min}$	0.625	1 symbol	7
CIOD [10]	$8N$	$\frac{1}{17.6678}d^2_{\min}$	1	2 symbols	6
QSTBC	$8N$	$\frac{1}{6}d^2_{\min}$	0.75	2 symbols	6
LTAST	$8N$	$\frac{1}{8}d^2_{\min}$	1	8 symbols	0
SAST	$8N$	$\frac{1}{8}d^2_{\min}$	1	4 symbols	4

LTAST codes (or DST codes), for (M, N) MIMO systems with M transmit and N receive antennas (see Tables I and II). The compared parameters are the diversity gain (G_d), coding gain[3] (G_c), code rate (R, in symbol pcu), number of symbols to be jointly ML detected, and degree of orthogonality (DO). The DO is defined as the minimum number of columns of codeword matrix that a column is orthogonal with.

SAST codes have the same coding gains compared to those of rate-one LTAST codes; however, the distance spectrum of SAST codes is much improved. For example, a computer search showed that for the codes designed for four transmit antennas and 4-QAM, the numbers of the codeword pairs having a minimum distance (coding gain) of SAST codes and the LTAST codes are 2560 and 7104, respectively. Hence, the performance of the former is significantly better than that of the latter. The simulation results in the next section will support this theoretical analysis.

[3]Note that the optimal signal rotation for the double-symbol decodable CIOD code in [10] is unknown. The best coding gain of this code with a 4-QAM signal is suggested in [25].

IV. SIMULATION RESULTS

A. Performance Results

In this section, we compare the performance of SAST codes and other STBC with rate of one symbol pcu or less. Unless stated otherwise, the BER curves are obtained by ML detection. Gray bit mapping is applied for all constellations.

Fig. 3 plots the BER of the SAST and LTAST codes for a $(4, 1)$ system using 4-, 16- and 64-QAM (with spectral efficiencies 2, 4, and 6 bits pcu accordingly). The SNR gain of SAST codes over that of the LTAST codes is substantial. For example, the SNR gain is about 1.3, 2, and 2.5 dB for 2, 4, and 6 bits pcu, respectively. The gains increase with the spectral efficiency.

Similar gains can be observed for higher numbers of transmit antennas. Fig. 4 compares the BER of the SAST and LTAST codes for a $(8, 1)$ system. Again, SAST codes outperform the LTAST codes. The SNR gain is 0.7 and 1.3 dB with 2 and 4 bits pcu, respectively.

In Fig. 5, the BER of SAST, γ-circulant, and CIOD codes in Tables I and II are compared. With four and eight transmit antennas, SAST codes outperform the other two codes.

The performances of SAST and QSTBC [7], [9] are compared in Fig. 6. When $M = 4$, the two codes have the same rate-one symbol pcu and perform identically. However, if

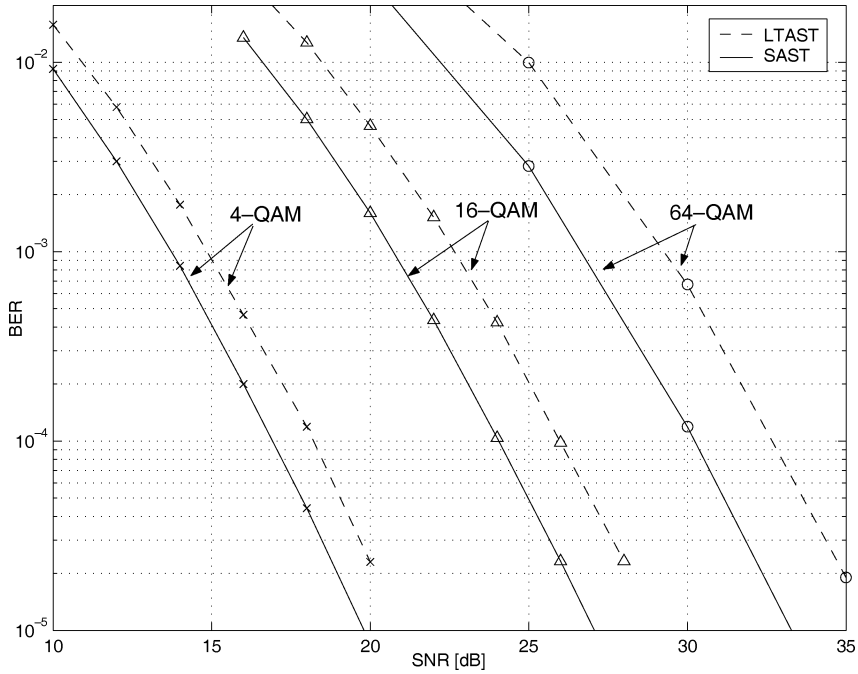

Fig. 3. Performance comparison of SAST and LTAST codes with $M = 4$ and $N = 1$.

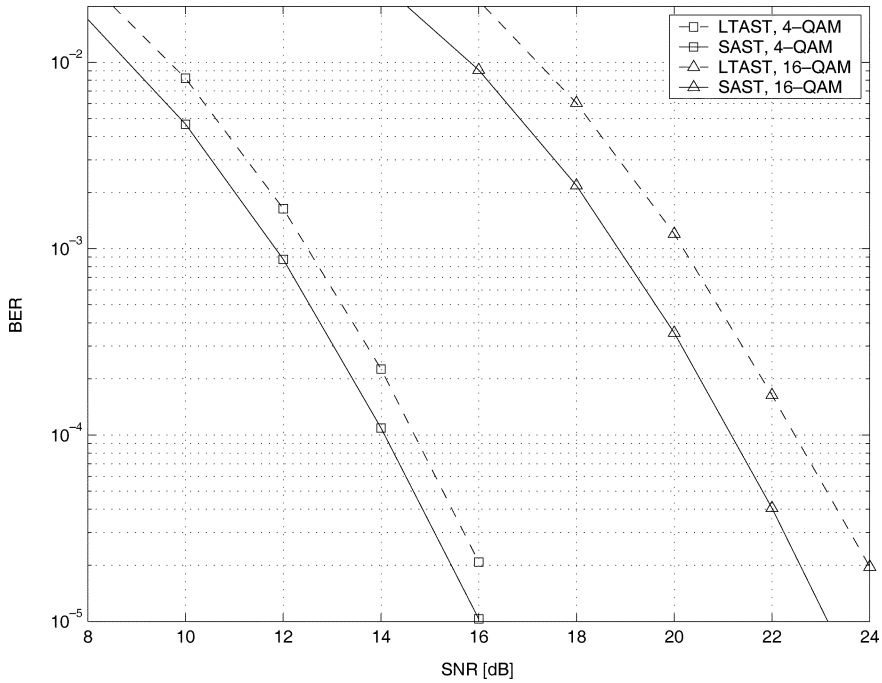

Fig. 4. Performance comparison of SAST and LTAST codes with $M = 8$ and $N = 1$.

$M = 6$, and the code rate of QSTBC is $3/4$, then we use 16-QAM for the QSTBC codes and 8-hexagonal constellation (8-HEX) [18] for SAST codes (optimal coding gain for $M = 6$) so that the two codes have the same 3 bits pcu. Fig. 6 shows that SAST codes produce about a 1.2-dB gain over the QSTBC codes. This performance gain of the SAST codes can be explained by examining the minimum Euclidean distances $d_{\min}$ of 8-HEX and 16-QAM, which are 0.9631 and 0.6325, respectively. Clearly, SAST codes have better spectral efficiency than that of the QSTBC codes; SAST codes can perform better than the QSTBC for six transmit antennas by using smaller constellations with a larger minimum Euclidean distance. This result can be extended for other cases when the number of transmit antennas is five or more.

While our theoretical analysis is carried out for even numbers of transmit antennas, SAST codes for an odd number of transmit antennas can be obtained by deleting one column of the SAST codewords (or switching off one transmit antenna) and by setting the channel gain associated with the switched-off antenna to zero at the decoder.

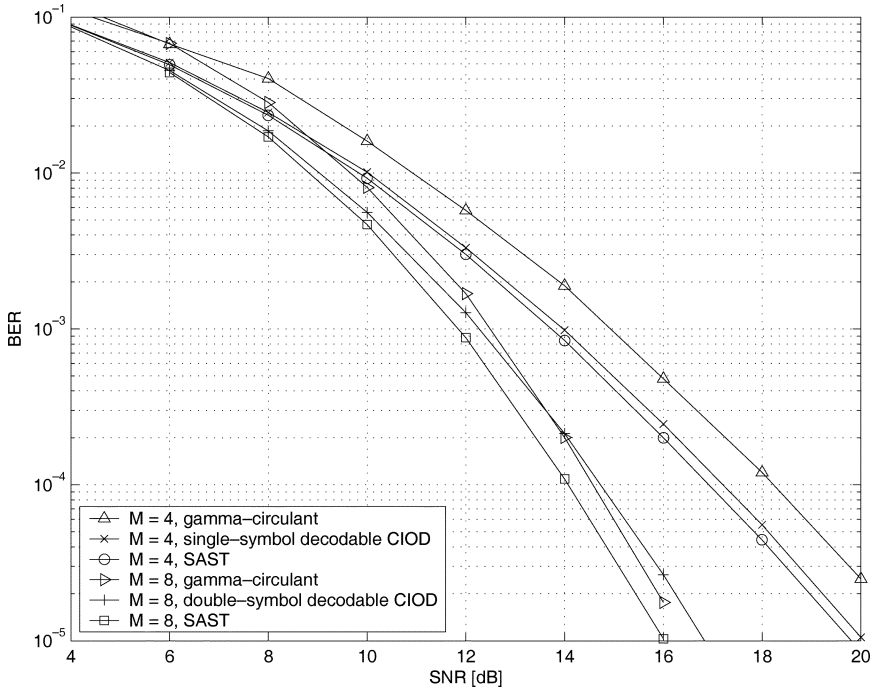

Fig. 5. Performance comparison of SAST, CIOD, and γ-circulant codes with 4-QAM (2 bits pcu), for $M = 4, 8$ and $N = 1$.

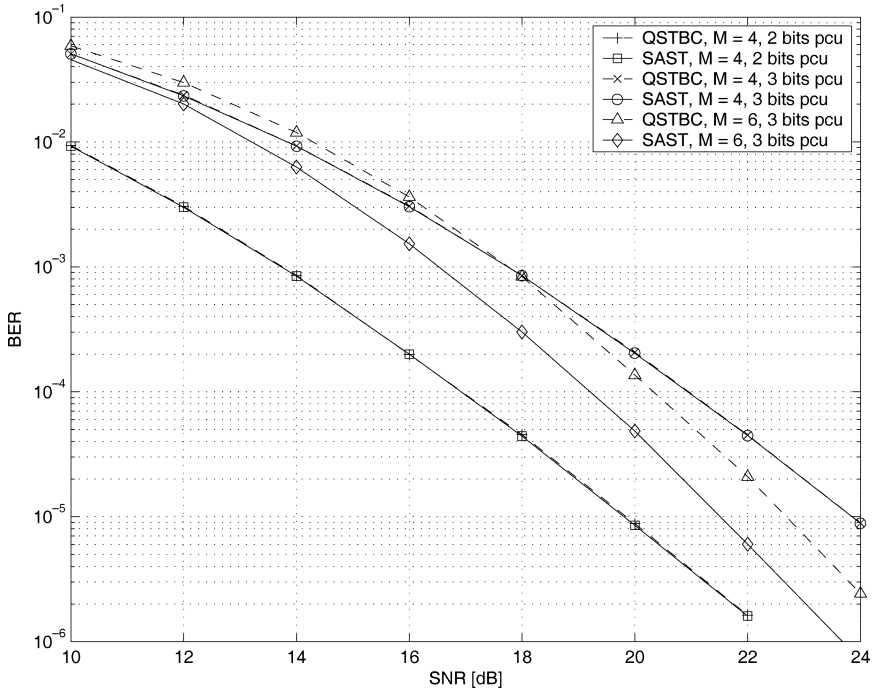

Fig. 6. Performance comparison of SAST and QSTBC codes with 2 and 3 bits pcu, for $M = 4, 6$, $N = 1$.

Fig. 7 illustrates the performance of SAST codes and the ST linear constellation precoding (ST-LCP) codes [12] with the same 2 bits pcu (4-QAM). The ST-LCP codes, in fact, are equivalent to DAST codes proposed in [11]; by using fast Fourier transform (FFT), one can convert the LTAST codes to the DAST codes (see [13] and property P4) of the circulant matrices in Section II-C). The slopes of the BER curves of the SAST and ST-LCP codes are almost parallel, indicating that the former achieve full diversity. Furthermore, notable gains of 1 and 1.5 dB over the ST-LCP codes are obtained for $M = 3$ and $M = 5$, respectively. Thus, SAST codes perform better compared to the LTAST codes for any number of transmit antennas.

Fig. 8 compares the performance of SAST, ST-LCP and linear dispersion (LD) codes [23] for spectral efficiency 2 and 6 bits pcu (4- and 64-QAM, respectively) and with $M = 3$ and $N = 1$. Fig. 8 shows that SAST codes perform better than the ST-LCP codes for all bit rates. SAST codes also perform better than the LD code with the same delay $T = 4$. With 2 and 6 bits

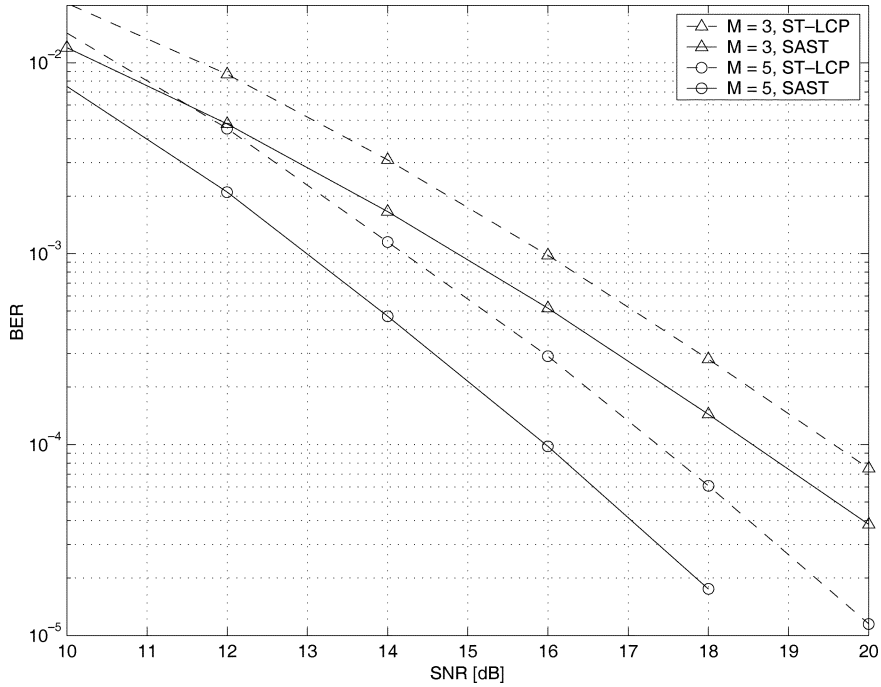

Fig. 7. Performance comparison of SAST and ST-LCP codes with 4-QAM, $M = 3, 5$, $N = 1$.

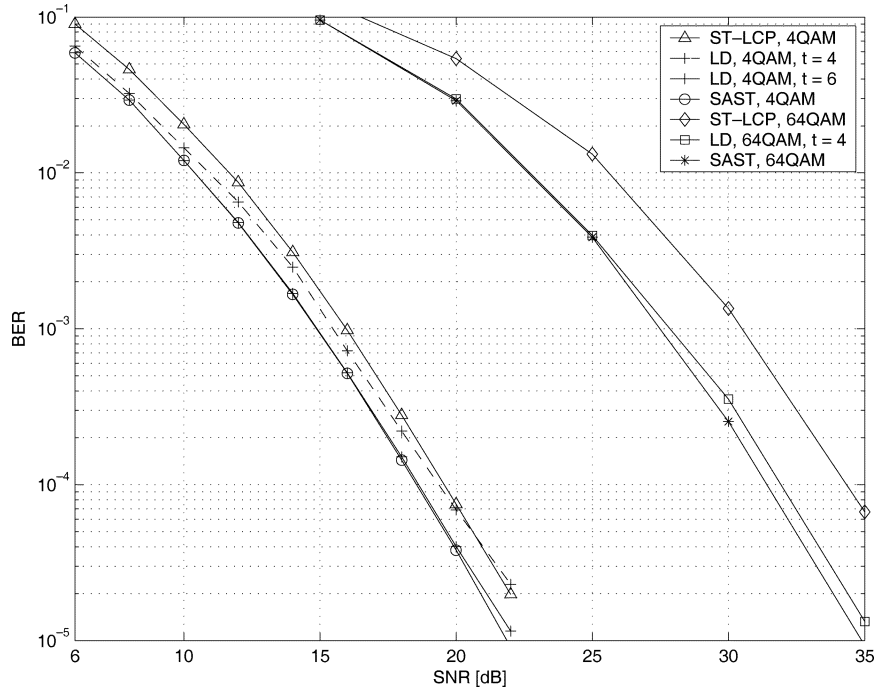

Fig. 8. Performance comparison of SAST, ST-LCP, and LD codes with 4- and 64-QAM, $M = 3$, $N = 1$.

pcu, SAST codes gain about 0.4 and 0.7 dB over the LD codes at BER 10^{-4}. With a higher delay design $T = 6$ and for 2 bits pcu, SAST codes perform the same as LD codes at a low SNR, but slightly better at high SNR. SAST codes improve over the LD codes because the design criterion of the LD codes aims at maximizing the mutual information. Hence, LD codes may not achieve full diversity, which may lead to inferior performance at high SNR. Note that the decoding complexity of the LD codes is always higher than that of SAST codes.

We have investigated the error-rate performance of SAST codes. The results show that they outperform CIOD, LTAST, γ-circulant, ST-LCP/DAST, QSTBC, and LD codes. Since the performance of OSTBC codes is inferior to that of these codes [9], [11], [12], [23], SAST codes also outperform OSTBC codes.

In some applications, suboptimal detectors may be employed to reduce the detection complexity. We thus examine the performance of LTAST and SAST codes with 16-QAM by using the

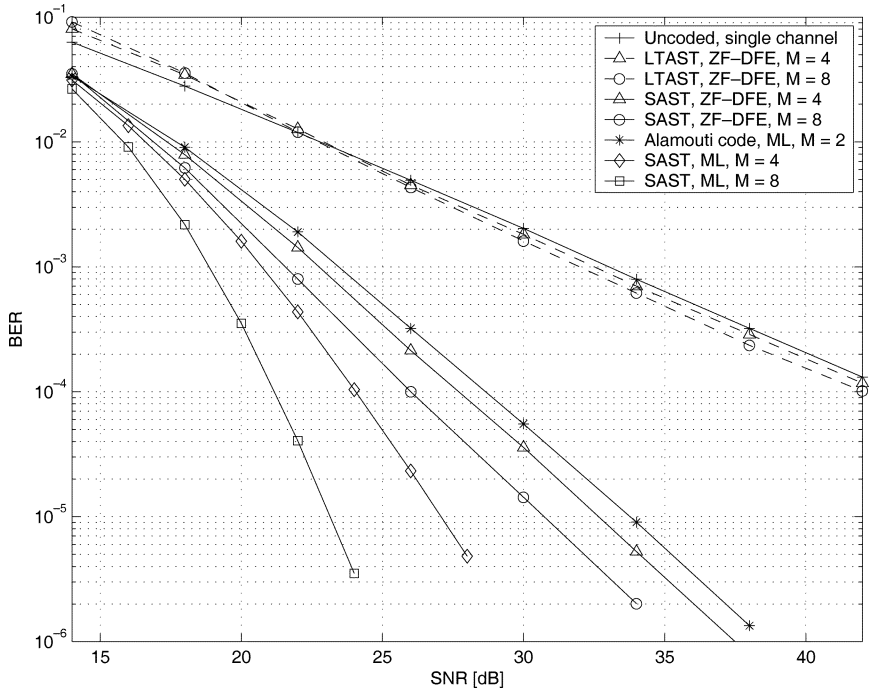

Fig. 9. Performance comparison of SAST and LTAST codes using V-BLAST optimal nulling and cancellation (or ZF-DFE for short) receiver for 16-QAM, $M = 4, 8$, $N = 1$.

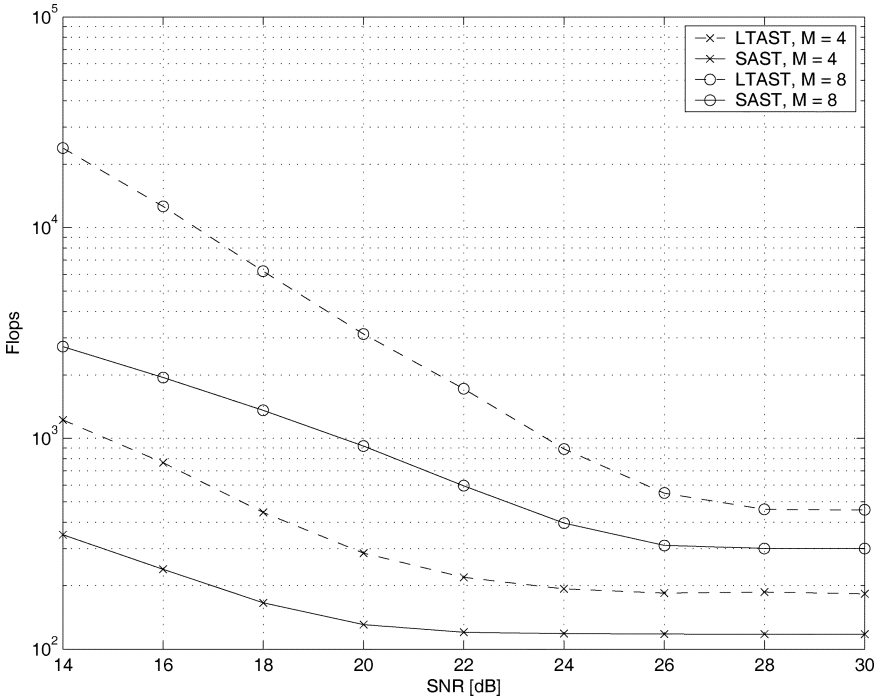

Fig. 10. Comparison of ML detection complexity of SAST and LTAST codes with sphere decoders for 16-QAM, $M = 4, 8$ and $N = 1$.

V-BLAST optimal nulling and a cancellation receiver or an optimal zero-forcing decision feedback equalization (ZF-DFE) receiver [21]. Fig. 9 depicts the performance of the two codes with such receiver. The BER of SAST codes with $M = 2$ (Alamouti code) and $M = 4, 8$ when using the sphere decoder, and the uncoded BER over a single Rayleigh fading channel, are also presented for comparison. By comparing the slopes of the BER curves, we can conclude that with the V-BLAST ZF-DFE receiver, SAST codes achieve a diversity order of 2, while the diversity order of the LTAST codes is only 1; moreover, the SAST codes yield a much better BER than that of the LTAST codes. With the ZF-DFE receiver, the LTAST codes produce a marginal gain compared with that of the uncoded data transmitted over a single Rayleigh fading channel ($M = N = 1$). On the other hand, the SAST codes with $M = 4$ and 8 gain about 1 and 2.9 dB, respectively, compared to the Alamouti code. With the

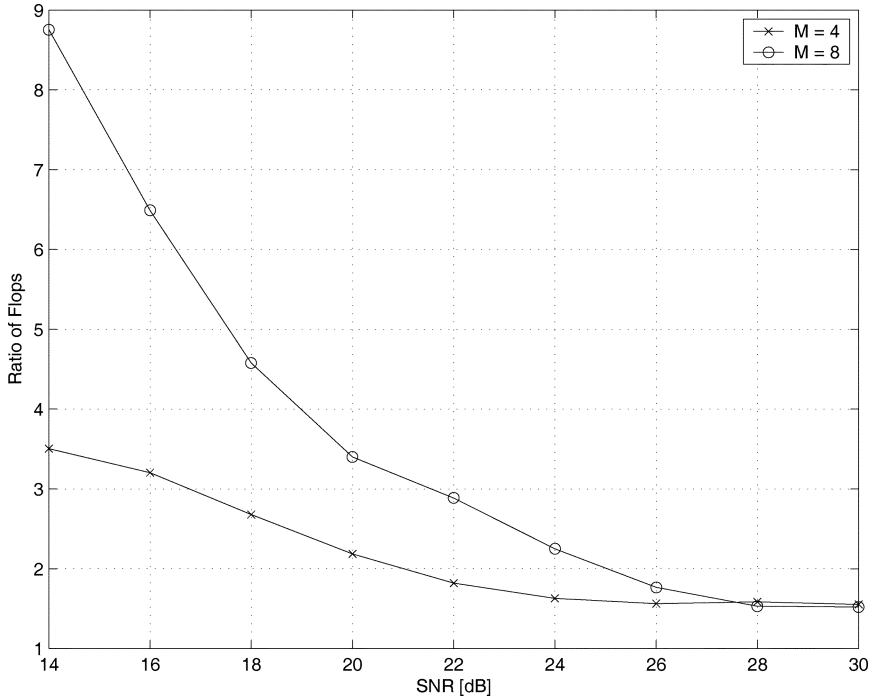

Fig. 11. Ratio of average numbers of flops used by sphere decoders for ML detection of LTAST and SAST codes for 16-QAM, $M = 4, 8$ and $N = 1$.

ZF-DFE receiver, the diversity order of SAST codes is only 2, but the code still delivers a notable coding gain.

B. Complexity Comparison

We present the average number of flops $F_L(\rho)$ and $F_S(\rho)$ used by the sphere decoders to detect the transmitted symbols of LTAST and SAST codes, respectively, as a metric of complexity measure. Note that the two sphere decoders can be run in parallel for decoding the SAST code, greatly decreasing the decoding time. The computations required by the preprocessing stage are not included. Fig. 10 plots $F_L(\rho)$ and $F_S(\rho)$ for the systems using 16-QAM with $M = 4, 8$ and $N = 1$. For a better illustration, the ratio $F_L(\rho)/F_S(\rho)$ is plotted in Fig. 11. The computation savings of the SAST codes compared with those of the LTAST codes are significant, especially at low and medium SNR ranges. This saving increases sharply with the number of transmit antennas. For example, at 16 dB, the computational complexity decreases 2.2 and 3.4 times for $(4, 1)$ and $(8, 1)$ systems.

V. Conclusion and Remarks

We derived a new class of ST block codes called SAST codes. They are full diversity, rate one (symbol pcu), and delay optimal for an even numbers of transmit antennas. The key design of SAST codes involves the block circulant structure, where the commutative property is exploited to reduce the decoding complexity. Compared with rate-one LTAST codes, SAST codes not only significantly reduce the detection complexity, but also give remarkable SNR gain of several decibels. SAST codes also outperform other STBC codes. Even when using the V-BLAST nulling and cancellation receiver, SAST codes perform much better than the LTAST codes and also outperform the Alamouti code. Note that this comparison is somewhat unfair as the Alamouti code uses only two transmit antennas. However, LTAST codes with the VBLAST suboptimal decoder could not perform better than the Alamouti code.

The construction of SAST codes can be extended in some ways. For example, since the code matrices of DAST [11], [12] and γ-circulant [15] codes are commutative, we can construct SAST codes by using these two codes.

Damen *et al.* [13, Prop. 4] showed that full-rate (designed for $N \geq M$) or rate-one (designed for $N = 1$) LTAST codes when concatenated with a *Gaussian codebook* and ML decoding achieve the optimal diversity multiplexing tradeoff (DMT) [26]. Additionally, Shashidhar *et al.* showed that the lower bound on D-MT of STBC from division algebras (including rate-one γ-circulant codes) is very close to the optimal D-MT for the MISO channel [27]. Since the SAST codes can be constructed from these two codes, and also because of our simulation results, where the data rate of SAST codes approximately increases 2 bits per 6 dB of SNR increment (cf., Figs. 3 and 4), we may predict that SAST codes with QAM achieve the optimal DMT for MISO channels [26], [28]. This observation needs to be analytically proved. Nevertheless, in terms of maximum mutual information, the use of SAST codes is nearly optimal for MISO channels. Hence, the SAST codes may be a good choice for the downlink of a mobile wireless system, where the base stations can be equipped with multiple transmit antennas, and the mobile handsets are equipped with only one receive antenna because of size/cost constraints.

Acknowledgment

The authors would like to thank anonymous reviewers for their constructive comments, which significantly improved the quality and presentation of this paper.

REFERENCES

[1] S. Parker, M. Sandell, M. S. Yee, Y. Sun, M. Ismail, P. Strauch, and J. McGeehan, "Space-time codes for future WLANs: Principles, practice, and performance," *IEEE Commun. Mag.*, vol. 42, no. 12, pp. 96–103, Dec. 2004.

[2] S. M. Alamouti, "A simple transmitter diversity scheme for wireless communication," *IEEE J. Sel. Areas. Commun.*, vol. 16, no. 8, pp. 1451–1458, Oct. 1998.

[3] V. Tarokh, H. Jafarkhani, and A. R. Calderbank, "Space-time block codes from orthogonal designs," *IEEE Trans. Inf. Theory*, vol. 45, no. 4, pp. 1456–1466, Jul. 1999.

[4] Z. A. Khan and B. S. Rajan, "Single-symbol maximum likelihood decodable linear STBCs," *IEEE Trans. Inf. Theory*, vol. 52, no. 5, pp. 2062–2091, May 2006.

[5] X.-B. Liang, "Orthogonal designs with maximal rates," *IEEE Trans. Inf. Theory*, vol. 49, no. 10, pp. 2468–2503, Oct. 2003.

[6] V. Tarokh, N. Seshadri, and A. R. Calderbank, "Space-time codes for high data rate wireless communication: Performance analysis and code construction," *IEEE Trans. Inf. Theory*, vol. 44, no. 2, pp. 744–765, Mar. 1998.

[7] H. Jafarkhani, "A quasi-orthogonal space-time block code," *IEEE Trans. Commun.*, vol. 49, no. 1, pp. 1–4, Jan. 2001.

[8] O. Tirkkonen, A. Boariu, and A. Hottinen, "Minimal nonorthogonality rate 1 space-time block code for 3+ Tx antennas," in *Proc. IEEE 6th Int. Symp. Spread-Spectrum Tech. Appl.*, Parsippany, NJ, Sep. 2000, pp. 429–432.

[9] W. Su and X.-G. Xia, "Signal constellations for quasi-orthogonal space-time block codes with full diversity," *IEEE Trans. Inf. Theory*, vol. 50, no. 10, pp. 2331–2347, Oct. 2004.

[10] Z. A. Khan, B. S. Rajan, and M. H. Lee, "On single-symbol and double-symbol decodable STBCs," in *Proc. IEEE Int. Symp. Inf. Theory*, Yokohama, Japan, Jun./Jul. 2003, p. 127.

[11] M. O. Damen, K. Abed-Meraim, and J. -C. Belfiore, "Diagonal algebraic space-time block codes," *IEEE Trans. Inf. Theory*, vol. 48, no. 3, pp. 628–636, Mar. 2002.

[12] Y. Xin, Z. Wang, and G. B. Giannakis, "Space-time diversity systems based on linear constellation precoding," *IEEE Trans. Wireless Commun.*, vol. 2, no. 2, pp. 294–309, Mar. 2003.

[13] M. O. Damen, H. E. Gamal, and N. C. Beaulieu, "Linear threaded algebraic space-time constellations," *IEEE Trans. Inf. Theory*, vol. 49, no. 10, pp. 2372–2388, Oct. 2003.

[14] P. J. Davis, *Circulant Matrices*, 1st ed. New York: Wiley, 1979.

[15] B. A. Sethuraman, B. S. Rajan, and V. Shashidhar, "Full-diversity, high rate space-time block codes from division algebras," *IEEE Trans. Inf. Theory*, vol. 49, no. 10, pp. 2596–2616, Oct. 2003.

[16] M. Rupp and C. F. Mecklenbrauker, "On extended Alamouti schemes for space-time coding," in *Proc. 5th Int. Symp. Wireless Personal Multimedia Commun.*, Oct. 2002, pp. 115–119.

[17] N. Sharma and C. B. Papadias, "Full-rate full-diversity linear quasi-orthogonal space-time codes for any number of transmit antennas," *EURASIP J. Appl. Signal Process.*, vol. 9, pp. 1246–1256, Aug. 2004.

[18] G. J. Foschini, R. D. Gitlin, and S. B. Weinstein, "Optimization of two-dimensional signal constellations in the presence of Gaussian noise," *IEEE Trans. Commun.*, vol. 22, no. 1, pp. 28–38, Jan. 1974.

[19] M. O. Damen, H. El Gamal, and G. Caire, "On maximum-likelihood detection and the search for the closest lattice point," *IEEE Trans. Inf. Theory*, vol. 49, no. 10, pp. 2389–2402, Oct. 2003.

[20] R. A. Horn and C. R. Johnson, *Matrix Analysis*. Cambridge, U.K.: Cambridge Univ. Press, 1985.

[21] G. D. Golden, G. J. Foschini, R. A. Valenzuela, and P. W. Wolniansky, "Detection algorithm and initial laboratory results using the V-BLAST space-time communication architecture," *IEE Electron. Lett.*, vol. 35, pp. 14–15, Jan. 1999.

[22] I. E. Telatar, "Capacity of multiantenna Gaussian channel," *Eur. Trans. Telecommun.*, vol. 10, pp. 585–595, Nov./Dec. 1999.

[23] B. Hassibi and B. M. Hochwald, "High-rate codes that are linear in space and time," *IEEE Trans. Inf. Theory*, vol. 48, no. 7, pp. 1804–1824, Jul. 2002.

[24] G. J. Foschini, D. Chizhik, M. Gans, C. Papadias, and R. A. Valenzuela, "Analysis and performance of some basic space-time architectures," *IEEE J. Sel. Areas. Commun.*, vol. 21, no. 3, pp. 303–320, Apr. 2003.

[25] C. Yuen, Y. L. Guan, and T. T. Tjhung, "A class of four-group quasi-orthogonal space-time block code achieving full rate and full diversity for any number of antennas," in *Proc. IEEE Personal Indoor Mobile Radio Commun. Symp.*, Berlin, Germany, Sep. 2005, pp. 92–96.

[26] L. Zheng and D. N. C. Tse, "Diversity and multiplexing: A fundamental tradeoff in multiple-antenna channels," *IEEE Trans. Inf. Theory*, vol. 49, no. 5, pp. 1073–1096, May 2003.

[27] V. Shashidhar, B. S. Rajan, and P. V. Kumar, "Asymptotic-information-lossless designs and the diversity-multiplexing tradeoff," *IEEE Trans. Inf. Theory*, vol. 55, no. 1, pp. 255–268, Jan. 2009.

[28] H. Yao and G. W. Wornell, "Structured space-time block codes with optimal diversity-multiplexing tradeoff and minimum delay," in *Proc. IEEE Global Telecommun. Conf.*, San Francisco, CA, Dec. 2003, pp. 1941–1945.

Ngoc-Dũng Đào (S'02–M'07) received the B.Eng. degree in communications engineering from Hanoi University of Technology, Hanoi, Vietnam, in 1995, the M.Eng. degree in telecommunications from Asian Institute of Technology (AIT), Pathumthani, Thailand, in 2002, and the Ph.D. degree in electrical and computer engineering from the University of Alberta, Edmonton, AB, Canada, in 2006.

He was with Siemens Information and Communications Networks Vietnam and held various technical positions from 1995 to 2001. From 2001 to 2003, he was Service Development Manager and then Sales Support Manager of NTC Co. Ltd. Vietnam. He was a Postdoctoral Research Fellow at McGill University, Montreal, QC, Canada, in 2007. Since December 2007, he has been with Telecommunications Research Laboratory, Toshiba Research Europe, Ltd., Bristol, U.K., where he is currently Senior Research Engineer. His recent research interests include multiple-input–multiple-output (MIMO) signal precessing (space–time coding, detection, single and multiuser precoding), multicarrier transmission techniques, error control coding, interference management, and avoidance in wireless networks.

Dr. Đào serves as a Cochair for the Multiple Antenna Systems and Space-Time Processing Track, IEEE Vehicular Technology Conference Fall 2010, Ottawa, ON, Canada.

Chintha Tellambura (SM'02) received the B.Sc. degree (with first-class honors) from the University of Moratuwa, Moratuwa, Sri Lanka, in 1986, the M.Sc. degree in electronics from the University of London, London, U.K., in 1988, and the Ph.D. degree in electrical engineering from the University of Victoria, Victoria, BC, Canada, in 1993.

He was a Postdoctoral Research Fellow with the University of Victoria, from 1993 to 1994 and with the University of Bradford, West Yorkshire, U.K., from 1995 to 1996. From 1997 to 2002, he was with Monash University, Melbourne, Australia. He is currently a Professor with the Department of Electrical and Computer Engineering, University of Alberta, Edmonton, AB, Canada. His research interests include diversity and fading countermeasures, multiple-input–multiple-output (MIMO) systems and space–time coding, and orthogonal frequency-division multiplexing.

Prof. Tellambura is an Associate Editor for the IEEE TRANSACTIONS ON COMMUNICATIONS and an Area Editor for Wireless Communications Systems and Theory of the IEEE TRANSACTIONS ON WIRELESS COMMUNICATIONS. He was the Chair of the Communication Theory Symposium at the 2005 Global Telecommunications Conference, St. Louis, MO.